

Reactivity of Heterobimetallic Alkoxy-silyl and Siloxy Complexes in the Catalytic Dehydrogenative Coupling of Tin Hydrides

Pierre Braunstein* and Xavier Morise

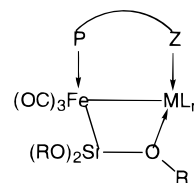
Laboratoire de Chimie de Coordination, Associé au CNRS (UMR 7513),
Université Louis Pasteur, 4 rue Blaise Pascal, F-67070 Strasbourg Cedex, France

Received April 25, 1997

Heterobimetallic complexes $[(OC)_3(R_3Si)Fe(\mu-dppm)Pd(\eta^3-allyl)]$ **1** ($R = OMe, Me, OSiMe_3, OSi(H)Me_2$) and $[(OC)_3Fe\{\mu-Si(OR)_2(OR)\}(\mu-dppm)PdCl]$ **6** ($R = Me, SiMe_3$) are effective catalyst in the dehydrogenative coupling of triorganotin hydrides $HSnR'_3$ ($R' = Ph, ^nBu$). Although the elementary transformations during catalysis appear to take place at palladium, the function of the iron fragment is to provide the palladium center with the appropriate coordination environment through metal–metal bonding and the Si-containing ligand. Indeed, complexes **1** and **6** revealed a higher catalytic activity than mononuclear Pd catalysts. Modifications of the substituents at silicon resulted in considerable variations of the TON (turnover number) and TOF (turnover frequency) values as well as in the lifetime of the catalysts. In the case of siloxy derivatives, TON and TOF values higher than in the case of the alkoxy-silyl analogs have been obtained whereas the lifetime of the catalyst is much longer for the latter. Possible mechanisms which rationalize the role of the silicon ligand are discussed. Solvent effects have also been observed. One of the key features of these systems is the retention of the bimetallic nature of the catalyst. TON and TOF higher than 2×10^5 and $3 \times 10^7 h^{-1}$, respectively, have been obtained in the case of HSn^nBu_3 . The catalytic activity of **1** toward the dehydropolymerization of tin dihydrides has been tested.

Introduction

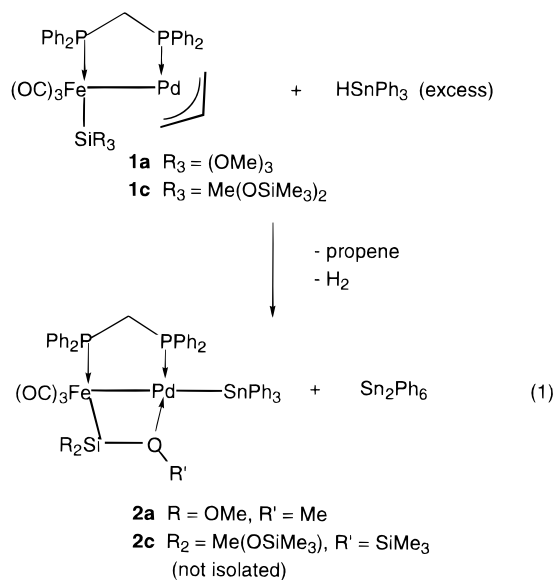
During the last few years, we have been interested in studying the properties of metal–silicon bonds in a heterobimetallic environment.^{1,2} This led to the discovery of a new class of complexes that display unusual Fe–Si–O–M four-membered rings involving the silicon backbone. The labile character of the dative oxygen–metal interaction, shown by VT ¹H NMR studies, may represent an interesting tool for catalytic purposes where the storage of a “masked” coordination site plays a key role.



We have already reported that treatment of $[(OC)_3\{(MeO)_3Si\}Fe(\mu-dppm)Pd(\eta^3-allyl)]$ **1a** ($dppm = Ph_2PCH_2PPh_2$) with excess $HSnPh_3$ afforded, *via* propene elimination, the trinuclear complex $[(OC)_3Fe\{Si(OMe)_2(O)Me\}(\mu-dppm)Pd(SnPh_3)]$ (**2a**), which is stabilized by an intramolecular Fe–Si–O–Pd four-membered ring (eq 1).^{1b} This reaction was also accompanied by evolution of H_2 and formation of Sn_2Ph_6 (*ca.* 10%). Interestingly when $HSnPh_3$ was added to a solution of $[(OC)_3\{(Me_3SiO)_2MeSi\}Fe(\mu-dppm)Pd(\eta^3-allyl)]$ **1c**, formation of the Fe–Pd–Sn complex **2c** was not evidenced. Instead a vigorous gas evolution and a complete transformation of $HSnPh_3$ into Sn_2Ph_6 occurred (eq 1). These observations clearly indicate that not only are complexes **1a** and **1c** catalysts (precursors) for the dehydrogenative tin–tin coupling of $HSnPh_3$, but that the nature of the

(1) (a) Braunstein, P.; Knorr, M.; Tiripicchio, A.; Tiripicchio Camellini, M. *Angew. Chem., Int. Ed. Engl.* **1989**, *28*, 1361. (b) Braunstein, P.; Knorr, M.; Piana, H.; Schubert, U. *Organometallics* **1991**, *10*, 828. (c) Braunstein, P.; Knorr, M.; Schubert, U.; Lanfranchi, M.; Tiripicchio, A. *J. Chem. Soc., Dalton Trans.* **1991**, 1507. (d) Braunstein, P.; Knorr, M.; Villarroya, E.; DeCian, A.; Fischer, J. *Organometallics* **1991**, *10*, 3714. (e) Knorr, M.; Braunstein, P. *Bull. Soc. Chem. Fr.* **1992**, 129, 663. (f) Knorr, M.; Faure, T.; Braunstein, P. *J. Organomet. Chem.* **1993**, *447*, C4. (g) Braunstein, P.; Faure, T.; Knorr, M.; Balegronne, F.; Grandjean, D. *J. Organomet. Chem.* **1993**, *462*, 271. (h) Braunstein, P.; Knorr, M.; Strampfer, M.; Tiripicchio, A.; Uguzzoli, F. *Organometallics* **1994**, *13*, 3038. (i) Knorr, M.; Braunstein, P.; Tiripicchio, A.; Uguzzoli, F. *Organometallics* **1995**, *14*, 4910. (j) Braunstein, P.; Knorr, M.; Stährfeldt, T. *J. Chem. Soc., Dalton Trans.* **1994**, 1913. (k) Braunstein, P.; Faure, T.; Knorr, M.; Stährfeldt, T.; DeCian, A.; Fischer, J. *Gazz. Chim. Ital.* **1995**, *125*, 35. (l) Braunstein, P.; Knorr, M. *J. Organomet. Chem.* **1995**, *500*, 21.

(2) Braunstein, P.; Morise, X.; Blin, J. *J. Chem. Soc., Chem. Commun.* **1995**, 1455.



silicon ligand strongly influences the course of the reaction.

The wide range of industrial^{3–6} and biological^{4–7} applications of hexaorganoditin compounds and their derived products has stimulated numerous studies toward their synthesis. They are usually obtained by various organic methods, such as condensation reactions of HSnR_3 with XSnR_3 ($X = \text{OH}, \text{NH}_2$, halide, OSnR_3, \dots),^{4–6,8,9} alkylations of tin halide derivatives,^{4–6,10} Wurtz-type reactions between XSnR_3 ($X = \text{halide}$) and metallic Li or Na,^{4–6,11} or reduction of bis(trialkyltin)-oxides.^{12,13} Surprisingly, the dehydrogenative coupling of HSnR_3 has been little studied. Only a few examples where this reaction is catalyzed by organometallic complexes have been described: $[\text{PdCl}_2(\text{MeCN})_2]$,¹⁴ $[\text{Pd}(\text{Ph})\text{I}(\text{PPh}_3)_2]$,¹⁴ $[\text{Pd}(\text{PPh}_3)_4]$,¹⁵ $[\text{Cp}'\text{Yb}(\mu\text{-H})_2]$ ¹⁶ ($\text{Cp}' = \text{C}_5\text{H}_4\text{Me}$), and $[\text{Ph}_3\text{PCuH}]_6$ ¹⁷ have been used, however,

low catalytic activities were reported for the Pd and Yb complexes, whereas in the case of the copper derivative the tin–tin dehydrogenative coupling was observed as a side reaction. It should also be mentioned that the dehydropolymerization of H_2SnR_2 in the presence of metallocene derivatives of Ti and Zr has been recently described.¹⁸

In the present paper, we wish to report investigations on the dehydrogenative coupling of stannanes catalyzed by heterobimetallic Fe–Pd alkoxysilyl and siloxy complexes. In addition to its intrinsic interest, we have used this reaction as a tool in order to study the influence of the heterobimetallic structure of the catalysts and of the ligand environment around the palladium center on the reaction process and provide an insight into homogeneous heterobimetallic catalysis.¹⁹ Some preliminary results have been communicated.²

Results

1. Synthesis of $[(\text{OC})_3\{\text{Me}_2\text{HSiO}\text{Me}_2\text{Si}\}\text{Fe}(\mu\text{-dppm})\text{Pd}(\eta^3\text{-allyl})]$ 1d. We have previously described the synthesis of heterobimetallic Fe–Pd silyl complexes **1a–c** by treatment of the dinuclear complex $[\text{Pd}(\eta^3\text{-C}_3\text{H}_5)(\mu\text{-Cl})_2]$ with 2 equiv of **4a–c** (obtained by deprotonation of the corresponding hydrido silyl complexes $[\text{HFe}(\text{SiR}_3)(\text{CO})_3(\text{dppm-}P)]$ (**3**), Scheme 1).^{1b,g} The new complex $[(\text{OC})_3\{\text{Me}_2\text{HSiO}\text{Me}_2\text{Si}\}\text{Fe}(\mu\text{-dppm})\text{Pd}(\eta^3\text{-allyl})]$ **1d** has been synthesized according to this procedure. The hydrido–silyl complex $\text{mer-}[\text{HFe}\{\text{SiMe}_2(\text{OSiHMe}_2)\}(\text{CO})_3(\text{dppm-}P)]$ (**3d**) was prepared by irradiation of a hexane solution of $[\text{Fe}(\text{CO})_5]$ and $(\text{Me}_2\text{HSi})_2\text{O}$ (ratio 1:4) followed by substitution of the carbonyl group trans to Si with dppm. Formation of the intermediate $\text{cis-}[\text{FeH}\{\text{SiMe}_2(\text{OSiHMe}_2)\}(\text{CO})_4]$ was monitored by IR spectrometry (see Experimental Section). The three $\nu(\text{CO})$ absorptions expected for a meridional arrangement of the CO ligands around the iron center

(3) Evans, C. J. *Chemistry of Tin*; Harrison, P. G., Ed.; Blackie: Glasgow, 1989; Chapter 13 and references cited therein.

(4) Davies, A. G.; Smith, P. G. *Comprehensive Organometallic Chemistry*; Wilkinson, G., Stone, F. G. A., Abel, E. W., Eds.; Pergamon: Oxford, 1982; Vol. 2, p 519 and references cited therein.

(5) Wardell, J.; Spencer, G. M. *Encyclopedia of Inorganic Chemistry*; King, R. B., Ed.; Wiley: New York, 1993; Vol. 8, p 4172 and references cited therein.

(6) Weis, R. W. *Organometallic Compounds*, 2nd ed.; Springer: New York, 1973; Vol. II, first supplement, pp 826–832 and references cited therein.

(7) Selwyn, M. J. *Chemistry of Tin*; Harrison, P. G., Ed.; Blackie: Glasgow, 1989; Chapter 11 and references cited therein.

(8) Glockling, F. *Chemistry of Tin*; Harrison, P. G., Ed.; Blackie: Glasgow, 1989; Chapter 8 and references cited therein.

(9) (a) Neumann, W. P.; Pedain, J. *Tetrahedron Lett.* **1964**, 2461. (b) Neumann, W. P.; Schneider, B. *Angew. Chem., Int. Ed. Engl.* **1964**, 3, 751.

(10) Wittig, G.; Meyer, E. J.; Lange, G. *Liebigs Ann. Chem.* **1951**, 571, 167.

(11) Grüttner, G. *Chem. Ber.* **1917**, 50, 1808.

(12) (a) Poller, R. C. *The Chemistry of Organotin Compounds*; Logos: London, 1970. (b) Neumann, W. P. *The Organic Chemistry of Tin*; Wiley: London, 1970. (c) Davies, A. G.; Osei-Kissi, D. K. *J. Organomet. Chem.* **1994**, 474, C8. (d) McAlonan, H.; Stevenson, P. J. *Organometallics* **1995**, 14, 4021 and references cited therein.

(13) Ulrich, S. (Witco GmbH) Ger. Offen. DE 4.231.083; *Chem. Abstr.* **1994**, 120, 245521v.

(14) Bugamin, N. A.; Gulevitch, Y. V.; Beletskaya, I. P. *Izv. Akad. Nauk. SSR, Ser. Khim.* **1982**, 11, 2639.

(15) (a) Mitchell, T. N.; Killing, H.; Rutschow, D. *J. Organomet. Chem.* **1986**, 304, 257. (b) Zhang, H. X.; Guibe, F.; Balavoine, G. *J. Org. Chem.* **1990**, 55, 1857 and references cited therein.

(16) Voskoboinikov, A. Z.; Beletskaya, I. P. *New J. Chem.* **1995**, 19, 723.

(17) Schubert, U.; Mayer, B.; Russ, C. *Chem. Ber.* **1994**, 127, 2189.

(18) (a) Imori, T.; Tilley, T. D. *J. Chem. Soc., Chem. Commun.* **1993**, 1607. (b) Imori, T.; Lu, V.; Cai, H.; Tilley, T. D. *J. Am. Chem. Soc.* **1995**, 117, 9931.

(19) Braunstein, P.; Rosé, J. *Comprehensive Organometallic Chemistry II*; Elsevier Science Ltd.: New York, 1995; Vol. 10, pp 351–85.

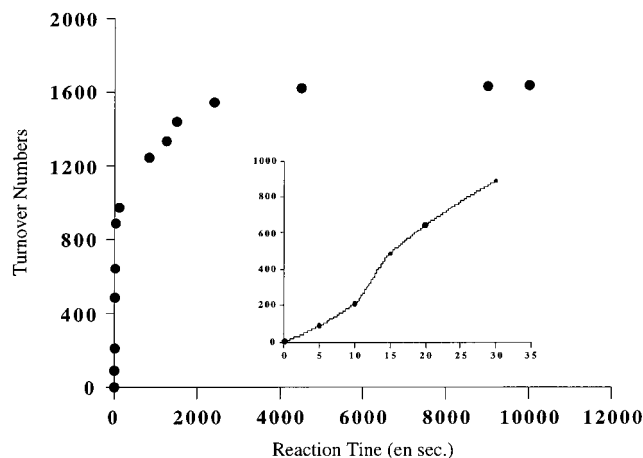


Figure 1. Evolution of the catalytic activity of **1c** in the formation of Sn_2Ph_6 from HSnPh_3 in dichloromethane; inset represents an expansion of the plot in the first 30 s of the reaction.

in **3d** are observed at 2050 (w), 1980 (s), and 1965 (vs) in the IR spectrum (toluene), whereas the ^1H NMR spectrum contains a doublet at $\delta -9.1$ ppm ($J_{\text{PH}} = 26$ Hz) and a signal at $\delta 5.0$ ppm characteristic of the Fe–H and Si–H groups, respectively. Compound **3d** was obtained as an air-sensitive sticky material that rapidly decomposes into the chelate complex $[\text{Fe}(\text{CO})_3(\text{dppm-}P,P)]$ after reductive elimination of silane.²⁰ It was, therefore, used as soon as prepared for subsequent reactions. Treatment of **3d** with 1 equiv of KH in THF followed by addition of the resulting mixture to a cold (233 K) THF solution of $[\text{Pd}(\eta^3\text{-C}_3\text{H}_5)(\mu\text{-Cl})_2]$ (0.5 mol equiv) yielded **1d** as an air-stable yellow-orange powder after purification by flash chromatography on alumina (eluent = Et_2O) (25% overall yield, based on dppm) (Scheme 1). Spectroscopic data are given in the Experimental Section.

2. Dehydrogenative Coupling of HSnPh_3 . *Note that all of the data refer to average values determined for at least three catalytic runs.* (i) **Fe–Pd Allyl Siloxy Catalysts.** Addition of a large excess (ca. 8000 mol equiv)²¹ of HSnPh_3 to a CH_2Cl_2 solution of **1c** (293 K) resulted in a vigorous gas evolution accompanied by an immediate color change from yellow to orange-red. After ca. 30 s, the gas evolution progressively decreased and finally ceased after ca. 1 h. During this time, the color of the mixture faded and a pale-yellow solution was obtained. The solvent was removed under vacuum, and Sn_2Ph_6 was precipitated by addition of Et_2O . Monitoring the volume of H_2 released allowed for a plot TON (turnover numbers) vs time to be made, which is shown in Figure 1. After a short induction period (see inset), the reaction rate reaches a maximum after ca. 10 s, which corresponds to a turnover frequency (TOF) of ca. $2 \times 10^5 \text{ h}^{-1}$. This maximum reaction rate is observed for only 5 s, after which a regular decrease leads, after ca. 50–60 min to a plateau. The latter corresponds to a TON of 1630; the same value was determined from the amount of Sn_2Ph_6 formed. Analysis of the combined residues from 5–6 experiments by

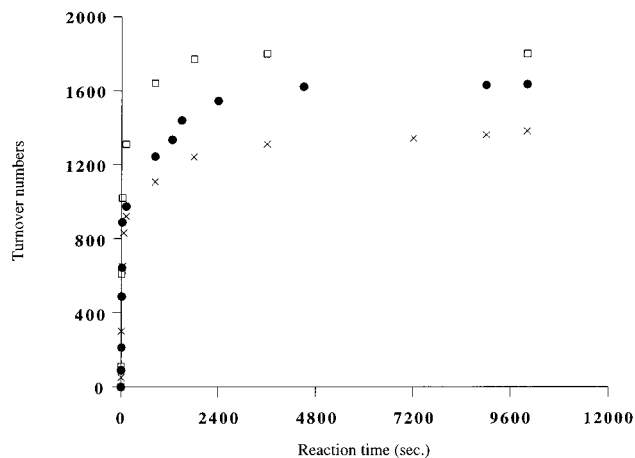


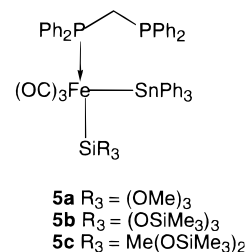
Figure 2. Comparison between the catalytic activities of the siloxyl complexes **1b** (x), **1c** (●) and **1d** (□) in the formation of Sn_2Ph_6 from HSnPh_3 in dichloromethane.

Table 1. Selected Catalysis Data for **1b**, **1c**, and **1d**

catalyst	TON max ^a	plateau, h ^b	TOF ^c
1b	1380	>1	1.15×10^5
1c	1630	1	1.98×10^5
1d	1800	0.5	2.16×10^5

^a Total catalytic activity expressed in turnover numbers (average value of a minimum of five experiments). ^b Time after which the plateau is reached. ^c Maximum turnover frequency expressed in turnovers per h.

^{31}P and ^1H NMR spectroscopic methods, after Sn_2Ph_6 had been separated, showed the presence of a set of signals ($^{31}\text{P}\{^1\text{H}\}$ NMR δ 43.62 (P(Fe), $J_{\text{PP}} = 44$ Hz, $J_{\text{P}^{119}\text{Sn}} = 169$ Hz, and $J_{\text{P}^{117}\text{Sn}} = 137$ Hz), -23.47 ($J_{\text{PP}} = 44$ Hz)) that we assigned to complex **5c** by comparison of these data with those of an authentic sample prepared by reaction of the anion **4c** with ClSnPh_3 .²² The Sn–P coupling observed in the downfield signal indicates a *cis* arrangement of these two nuclei about the Fe center, as represented below. However, this com-



pound was not isolated in pure form from these residues nor was any mononuclear Pd complex evidenced.

The siloxy complexes **1b** and **1d** are also efficient catalysts for the dehydrogenative coupling of HSnPh_3 . Under the reaction conditions reported above for **1c**, the volume of H_2 released was monitored in both cases (TON vs time, Figure 2). Selected catalysis data are reported in Table 1. The presence of complex **5b** in the combined residues of the different catalytic experiments using **1b** has been evidenced by $^{31}\text{P}\{^1\text{H}\}$ NMR. We have independently tested pure complexes **5a** (see below) or **5c** and observed no catalytic activity.

(ii) **Fe–Pd Allyl Alkoxysilyl Catalysts.** The above results prompted us to reinvestigate the reaction be-

(20) Formation of $[\{\text{Me}_2\text{Si}(\text{OMe}_2\text{Si})\}\text{Fe}(\text{CO})_3(\text{dppm-}P)]$ was never observed.

(21) The determination of these reaction conditions has been discussed in ref 2.

(22) Braunstein, P.; Charles, C. Unpublished results.

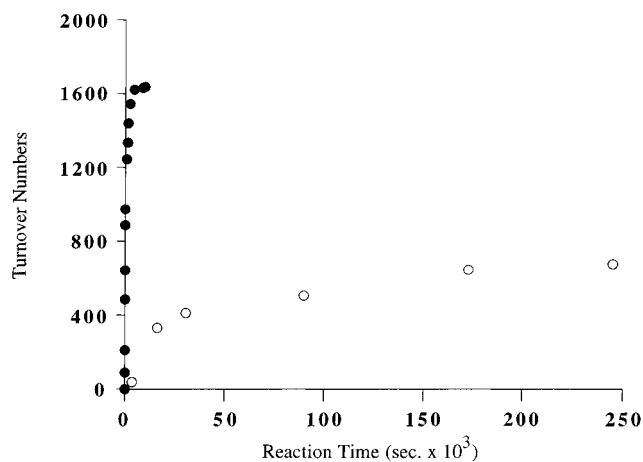


Figure 3. Comparison between the catalytic activities of **1a** (○) and **1c** (●) in the formation of Sn_2Ph_6 from HSnPh_3 in dichloromethane.

tween HSnPh_3 and the alkoxy-silyl complex **1a**^{1b} in order to evaluate the factors responsible for the large difference of reactivity between the latter and the siloxy complexes under similar reaction conditions. When a large excess of HSnPh_3 (ca. 8000 mol equiv) was added to a CH_2Cl_2 solution of **1a**, a very mild gas evolution was observed, accompanied by an immediate color change from yellow to red. The latter is characteristic of the formation of the trimetallic complex **2a**^{1b} (eq 1), which can be isolated (yield >80%) if the reaction is quenched after a few minutes by the addition of 2–3 drops of water. Contrary to what occurred in the case of complexes **1b–d**, the evolution of H_2 did not stop nor decrease after 1 h and was still observed after 48 h while a progressive fading of the color of the solution was noticed. Monitoring the formation of Sn_2Ph_6 (see Experimental Section) as a function of time gave the plot shown in Figure 3 (white dots (○)). Although the curve is similar to that obtained with **1c** (black dots (●)), the scale is by far different: the plateau is only reached after 48 h, which corresponds to a TON of 700. The TOF corresponding to the maximum activity of the catalyst, observed between 1 and 4.5 h, is lower than 100 h^{-1} . The combined pale yellow residues from 5–6 experiments, obtained after the solvent had been removed and Sn_2Ph_6 separated, were analyzed by $^{31}\text{P}\{^1\text{H}\}$ and ^1H NMR spectroscopic methods. Signals assignable to complex **5a** analogous to **5b** and **5c**²² were observed ($^{31}\text{P}\{^1\text{H}\}$ NMR δ 44.7 (P(Fe)), $J_{\text{PP}} = 45 \text{ Hz}$, $J_{\text{P}^{119}\text{Sn}} = 160 \text{ Hz}$, and $J_{\text{P}^{117}\text{Sn}} = 145 \text{ Hz}$), -23.1 ($J_{\text{PP}} = 45 \text{ Hz}$)), whereas no trace of **1a** or **2a** was evidenced. When the catalytic experiments were carried out with **2a** instead of **1a**, the same catalytic activity was observed.

(iii) Fe–Pd–Cl Catalysts. We have also tested the reactivity of $[(\text{OC})_3\text{Fe}\{\mu\text{-Si}(\text{OR})_2(\text{OR})\}(\mu\text{-dppm})\text{PdCl}]$ **6a** (R = Me)^{1a} and **6b** (R = SiMe_3)¹¹ toward the dehydrogenative coupling of HSnPh_3 . Interestingly, these two complexes exhibited the same catalytic activity as their Pd(allyl) analogs **1a** and **1b**, respectively. Furthermore the Fe–Pd–Sn complex **2a** was isolated in high yield (>80%) when the reaction with **6a** was quenched with water after a few minutes. This observation suggest a similar reaction mechanism for the Fe–Pd–Cl and Fe–Pd(allyl) catalysts.

Table 2. Catalytic Activity of Heterobimetallic Fe–Pd Alkoxy-silyl and Siloxy Complexes and Mononuclear Pd Complexes in the Dehydrogenative Coupling of HSnPh_3

Fe–Pd complexes		mononuclear Pd complexes	
catalyst	TON ^a	catalyst	TON ^a
1a	700	$[\text{Pd}(\eta^3\text{-allyl})(\mu\text{-Cl})_2]$ (13)	800
1b	1380	$\text{Pd}(\eta^3\text{-allyl})\text{Cl}(\text{PPh}_3)$ ^b (14)	860
1c	1630	$\text{PdCl}_2(\text{PhCN})_2$ (15)	300
1d	1800	$\text{Pd}(\text{mbd})\text{Cl}_2$ ^c (16)	370
2a	700	$\text{PdMeCl}(\text{P}\sim\text{O})_2$ ^d (17)	430
6a	700	$\text{Pd}(\text{OAc})_2$ (18)	460
6b	1380		

^a Total catalytic activity expressed in turnover numbers, determined from the mass of Sn_2Ph_6 recovered (average value of a minimum of five experiments); $T = 293 \text{ K}$, ratio $[\text{HSnPh}_3]/[\text{cat.}] = 8000$, solvent CH_2Cl_2 , reaction time = 3 h, except for **1a**, **2a**, and **6a** where reaction time = 96 h. ^b Formed *in situ* by addition of 2 equiv of PPh_3 to a solution of $[\text{Pd}(\eta^3\text{-allyl})(\mu\text{-Cl})_2]$. ^c mbd = norbornadiene. ^d $\text{P}\sim\text{O} = \text{Ph}_2\text{PCH}_2\text{C}(\text{O})\text{Ph}$.

Table 3. Selected Catalysis Data for the Dehydrocoupling of HSnPh_3 Catalyzed by **1c in Different Solvents**

solvent	TON max ^a	plateau, h ^b	TOF ^c
Et_2O , Tol, CH_2Cl_2 ^d	1600 ^e	1	ca. 2×10^5
THF	600	0.5	6.5×10^3
acetone	6800	3	8.9×10^3

^a Total catalytic activity expressed in turnover numbers (average value of a minimum of five experiments). ^b Time after which the plateau is reached. ^c Maximum turnover frequency expressed in turnovers per h. ^d In these solvents the catalytic activity was almost not modified. ^e Average value, Δ within $\pm 2\%$.

(iv) Mononuclear Palladium Complexes. We have determined the catalytic activity of a series of mononuclear Pd complexes²³ under the same experimental conditions as those reported above for the Fe–Pd heterobimetallic complexes. The TON determined from the quantities of Sn_2Ph_6 obtained are listed in Table 2. These values range from 300 for $[\text{PdCl}_2(\text{PhCN})_2]$ to 860 for $[\text{Pd}(\eta^3\text{-allyl})\text{Cl}(\text{PPh}_3)]$. In all cases the evolution of H_2 was over after 2 h, whereas the lifetime of the heterobimetallic catalysts varied from 0.5 to 72 h depending on the nature of the silyl group.

(v) Solvent Effects. The dehydrogenative coupling of HSnPh_3 catalyzed by **1c** has been carried out in various solvents with monitoring of the volumes of H_2 released. Selected catalysis data are reported in Table 3. Almost identical data have been determined when the reaction was carried out in Et_2O , toluene, or CH_2Cl_2 . However, it was much more sensitive to acetone and THF, as illustrated in Figure 4. The role of THF resembles that of a reaction inhibitor, whereas the efficiency and lifetime of the catalyst were enhanced in acetone. It is remarkable in this case that although a relatively low TOF (6800 h^{-1}) was observed, when compared to that obtained in solvents like Et_2O , toluene, and CH_2Cl_2 (ca. $2 \times 10^5 \text{ h}^{-1}$), the reaction proceeded at this rate for almost 1 h, whereas the maximum reaction rate was maintained for only a few seconds in the other cases. Higher catalytic activity and enhancement of the lifetime of the catalyst in acetone have also been observed for **1b** (Table 4).

(23) Fe complexes such as $[\text{Fe}_2(\text{CO})_9]$ in THF and $[\text{HFe}(\text{SiR}_3)(\text{CO})_3(\text{dppm-}P)]$ (R = OMe, OSiMe₃) have also been tested under similar conditions; they do not catalyze the dehydrogenative Sn–Sn coupling.

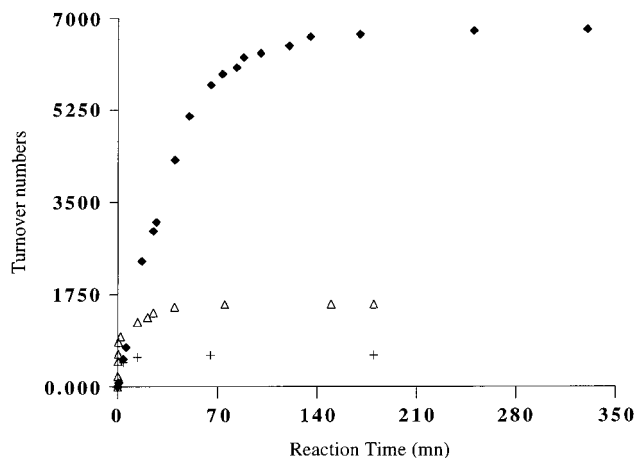


Figure 4. Catalytic activity of **1c** in the formation of $\text{Sn}_2\text{-Ph}_6$ from HSnPh_3 in Et_2O , CH_2Cl_2 , or toluene (Δ), acetone (\blacklozenge) and THF (+).

Table 4. Total Catalytic Activity and Reaction Time for the Dehydrogenative Coupling of HSnPh_3 Catalyzed by **1b and **1c** in Acetone and CH_2Cl_2**

catalyst	CH_2Cl_2		acetone	
	TON max ^a	RT, h ^b	TON max ^a	RT, h ^b
1b	1300	ca. 1.25	4380	ca. 3.5
1c	1630	1	6800	3

^a Total catalytic activity expressed in turnover numbers (average value of a minimum of five experiments). ^b RT = Reaction time corresponding to the end of gas evolution.

Table 5. Dehydrogenative Coupling of Tin Hydrides Catalyzed by **1a or/and **1b**^a**

tin hydride	catalyst	product (mn) ^b	TON max ^c
HSnPh_3	1a	Sn_2Ph_6 (60)	30
	1b	Sn_2Ph_6 (60)	1300
HSnBu_3	1a	Sn_2Bu_6 (3)	ca. 114 000
	1b	Sn_2Bu_6 (3)	ca. 202 000
H_2SnPh_2	1b	$[\text{SnPh}_2]_n$ ^d (60)	1100
$\text{H}_2\text{Sn}^n\text{Bu}_2$	1b	$[\text{Sn}^n\text{Bu}_2]_n$ and $\text{H}[\text{Sn}^n\text{Bu}_2]_n\text{H}$ ^d (120)	20 000

^a In CH_2Cl_2 ; T = 20 °C. ^b Reaction time in minutes. ^c Turnover numbers: average values of a minimum of three experiments/run. ^d Structure of oligomers not determined.

3. Dehydrogenative Coupling of HSnBu_3 . We have also evaluated the reactivity of **1a** and **1b** toward the dehydrogenative coupling of HSnBu_3 . Vigorous evolution of H_2 was observed upon addition of the catalysts to Et_2O (or CH_2Cl_2) solutions of the tin hydride (ratio $\text{HSnBu}_3/\text{cat.}$ ca. 1×10^6). The volume of H_2 released was monitored and converted into turnover numbers. The plot of turnover numbers vs time is given in Figure 5. In both cases a plateau is reached after 2–3 min, whereas much longer reaction times were observed in the case of HSnPh_3 . Note that further addition of catalyst after this period produced a vigorous gas evolution, thus showing that consumption of HSnBu_3 was not responsible for the loss of catalytic activity of **1a, b** and the short catalyst lifetime. Interestingly, very high TONs have been observed: 114 000 and 202 000 for **1a** and **1b**, respectively. These values are more than 150 times those determined for the same catalysts in the presence of HSnPh_3 . Furthermore, the TOFs are also amazingly high: ca. $2.3 \times 10^7 \text{ h}^{-1}$ for **1a** and ca. $3 \times 10^7 \text{ h}^{-1}$ for **1b**. It should be mentioned that these reactions were carried out in the dark and in the

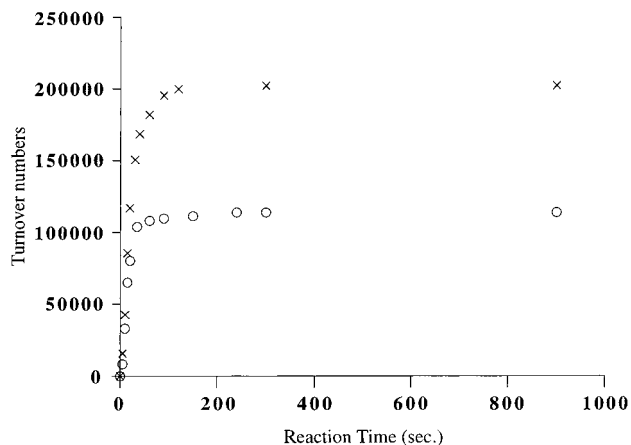


Figure 5. Comparison between the catalytic activities of **1a** (○) and **1b** (×) in the formation of Sn_2^nBu_6 from HSn^nBu_3 in dichloromethane.

presence of a radical scavenger (hydroquinone) and that no solvent effect was noticed.

4. Dehydrogenative Oligomerization of Tin Dihydrides. We have also tested the reactivity of complex **1b** toward the dehydrogenative oligomerization of tin dihydrides H_2SnR_2 (R = Ph, ⁿBu). Upon addition of **1b** to an Et_2O solution of $\text{H}_2\text{Sn}^n\text{Bu}_2$ (ratio $\text{H}_2\text{Sn}^n\text{Bu}_2/\mathbf{1b}$ = ca. 1×10^5), a vigorous evolution of H_2 was observed whose intensity rapidly decreased and ceased after 2 h. Assuming that 1 mol equiv of H_2 was released per catalytic cycle, a TON of ca. 20 000 was determined. In order to avoid the presence of a large excess of unreacted $\text{H}_2\text{Sn}^n\text{Bu}_2$ and thus facilitate analysis of the polystannanes obtained, the reaction was repeated using a $\text{H}_2\text{Sn}^n\text{Bu}_2/\mathbf{1b}$ ratio of ca. 25 000. When the reaction was over, the volatiles were removed under vacuum, affording a brown waxy residue. Its UV–vis spectrum (CH_2Cl_2 solvent) showed λ_{max} values at 380, 350, and 314 nm, however, the two former bands were of low intensity and a rapid photobleaching was observed, resulting in their disappearance. In the ¹¹⁹Sn NMR spectrum (benzene-*d*₆), several signals were observed between δ –164 and –203. On the basis of recently reported ¹¹⁹Sn NMR data,^{18b,24} the main resonance at δ –190 (broad signal) was assigned to linear $\text{H}(\text{Sn}^n\text{Bu}_2)_n\text{H}$ chains whereas weaker resonances at δ –201 and –203 correspond to the cyclic species *cyclo*-(Sn^nBu_2)₅ and *cyclo*-(Sn^nBu_2)₆, respectively. Other sig-

(24) Jousseau, B.; Noiret, N.; Pereyre, M.; Saux, A.; Francès, J.-M. *Organometallics* **1994**, *13*, 1034.

(25) See, for example: (a) Cauty, A. J. *Acc. Chem. Res.* **1992**, *25*, 83. (b) Cauty, A. J. *Platinum Met. Rev.* **1993**, *37*, 2. (c) Cauty, A. J. *Comprehensive Organometallic Chemistry II*; Abel, E. W., Stone, F. G. A., Wilkinson, G., Eds.; Elsevier: New York, 1994; Chapter 5 and references cited therein.

(26) (a) Woo, H. G.; Walzer, J. F.; Tilley, T. D. *J. Am. Chem. Soc.* **1992**, *114*, 7047. (b) Tilley, T. D. *Acc. Chem. Res.* **1993**, *26*, 22. (c) Imori, T.; Tilley, T. D. *Polyhedron* **1994**, *10*, 2231.

(27) (a) Jessop, P. G.; Morris, R. H. *Coord. Chem. Rev.* **1992**, *121*, 155. (b) Arndtsen, B. A.; Bergman, R. G.; Mobley, T. A.; Peterson, T. H. *Acc. Chem. Res.* **1995**, *28*, 154 and references cited therein. (c) Crabtree, R. H. *Acc. Chem. Res.* **1995**, *95*, 987. (d) Folga, E.; Woo, T.; Ziegler, T. In *Theoretical Aspects of Homogeneous Catalysis*; van Leeuwen, P. W. N. M., Morokuma, K., van Lenthe, J. H., Eds.; Kluwer: Dordrecht, 1995; p 115 and references cited therein.

(28) Milet, A.; Dedieu, A.; Kapteijn, G.; van Koten, G. *Inorg. Chem.* **1997**, *36*, 3223.

(29) (a) Roskamp, E. J.; Pedersen, S. F. *J. Am. Chem. Soc.* **1987**, *109*, 3152. (b) Carofiglio, T.; Floriani, C.; Roth, A.; Sgamellotti, A.; Rosi, M.; Chiesi-Villa, A.; Rizzoli, C. *J. Organomet. Chem.* **1995**, *488*, 141.

(30) We thank a reviewer for raising this question.

nals (δ -164, -174, -179, and -184) were not assigned. The ^1H NMR spectrum also indicated the presence of a mixture of linear $\text{H}(\text{Sn}^n\text{Bu}_2)_n\text{H}$ and cyclic $(\text{Sn}^n\text{Bu}_2)_n$ polystannanes (see Experimental Section). Analysis of a THF solution by GPC with a refractive index detector indicated a large mass distribution with $M_w/M_n = 55700/12800$ for the linear oligomers.

When $\text{R} = \text{Ph}$, a mild gas evolution was observed after addition of **1b** ($\text{H}_2\text{SnPh}_2/\mathbf{1b}$ ratio = ca. 10 000). It ceased after 1 h. A pale yellow-brown precipitate was formed, which was separated and washed with pentane affording a pale yellow solid. A TON of 1100 was determined on both the volume of H_2 released and the amount of polystannanes recovered, assuming that it was constituted of $[\text{SnPh}_2]_n$ species and that one Sn–Sn bond was formed per catalytic cycle. Mass spectroscopy only revealed the presence of Sn_nPh_m fragments with $1 \leq n \leq 6$ and $1 \leq m \leq 7$. A λ_{max} value of 350 nm was observed in the UV–vis spectrum, which corresponds to oligomers with $M_w/M_n = 1140/1100$ (GPC measurements), probably *cyclo*- $[\text{SnPh}_2]_n$ oligomers with $n = 4$ and 5.^{18,31} No discernible peaks assignable to Sn–H groups were detected in the ^1H NMR and IR spectra.

Discussion

Mechanistic Considerations for the Dehydrogenative Coupling of HSnPh_3 Catalyzed by Heterobimetallic Fe–Pd Silyl Complexes. The structure of complexes **1** (18 electron iron center and allyl ligand coordinated to the 16 electron palladium atom) along with the fact that mononuclear palladium complexes catalyze the dehydrogenative coupling of stannanes^{14,15} (see Table 2) strongly suggest that the elementary transformations during the catalysis take place at the palladium center, the iron fragment participating in its coordination environment through the metal–metal bonding, the bridging phosphine, and the silyl ligand.

We have found that **1a** and the trinuclear Fe–Pd–Sn complex **2a** exhibited the same catalytic activity in the dehydrogenative coupling of HSnPh_3 . We have previously reported that reaction of **1a** with HSnPh_3 led to the immediate formation of **2a**, *via* propene elimination.^{1b} We, therefore, assume that this reaction represents the initial step of the catalytic process studied here and may be responsible for the induction period observed in the plots shown in Figures 1 and 2. Although no siloxy analog of **2a** could be isolated, probably owing to the high reactivity of these species under the reaction conditions, nor prepared by an alternative route, the rapid transformation of complexes **1b–d** into Fe–Pd–Sn intermediates in the presence of HSnPh_3 is supported by the immediate color change of the reaction mixture upon addition of the stannane from yellow to red, the latter being the characteristic color of **2a**. It should also be mentioned that no modification of the kinetic parameters or TON values for the different catalysts has been noticed when the reactions were carried out in the presence of radical scavengers or/and in the dark, which seems to rule out a radical-chain mechanism. Furthermore, addition of Hg metal was

also noneffective, which is in agreement with a purely homogeneous catalytic process.

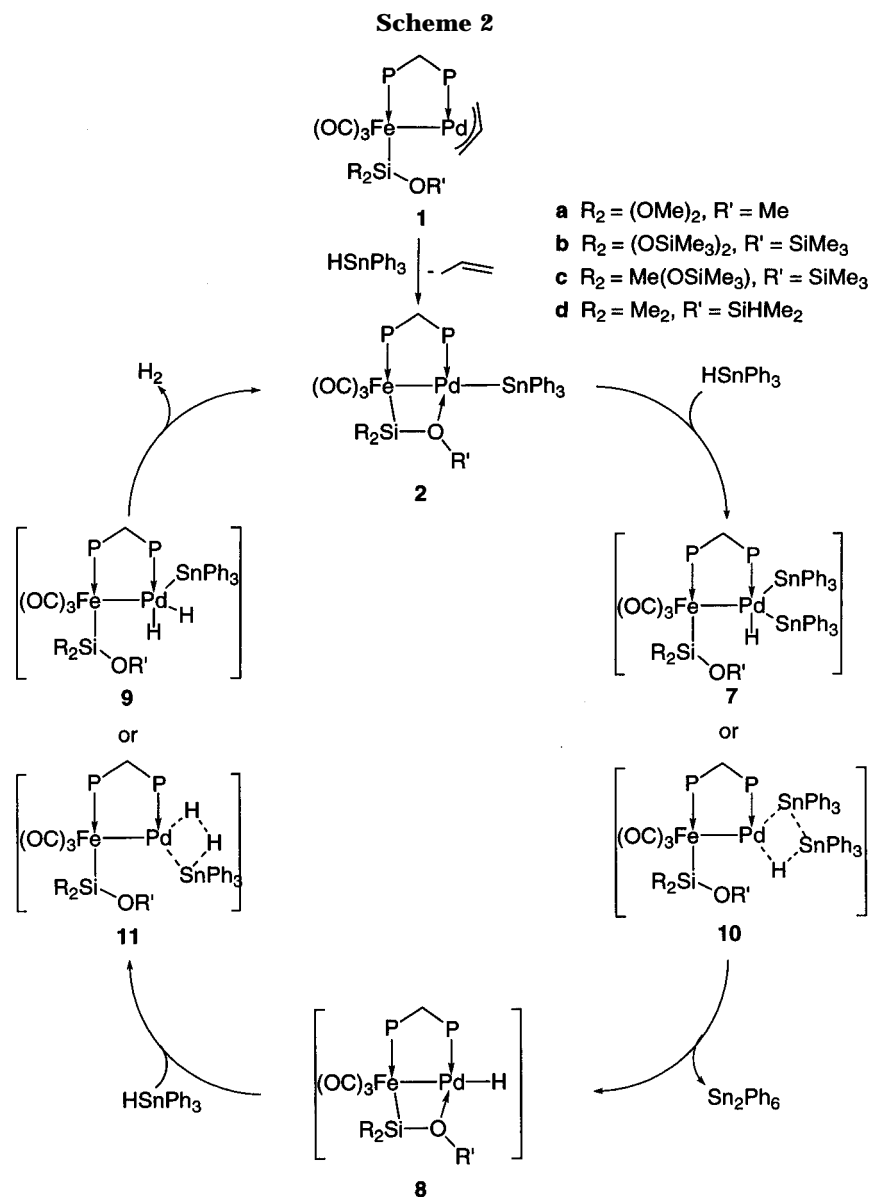
After the initial formation of the Fe–Pd–Sn species, we propose that the tin–tin dehydrogenative coupling reactions occur either by successive oxidative additions and reductive eliminations or by a σ -bond metathesis-type mechanism (Scheme 2). In both cases the hemilability of the bridging $\mu_2\text{-}\eta^2\text{-SiO}$ ligand is involved while the heterobimetallic structure is preserved. In the case of migratory insertions of small molecules (CO, CNR, olefins) into the M–C bond (M = Pd, Pt) of heterobimetallic alkoxy-silyl Fe–M complexes,^{1j} a mechanism also based on successive Fe–Si–O–M ring openings and closures resulting from the hemilability of the bridging -Si(OMe)_3 group has been described.

Intermediates **2** and **8** are stabilized by an intramolecular O \rightarrow Pd interaction. Opening of this Fe–Si–O–Pd four-membered ring releases a vacant coordination site at the Pd center, and this could be followed either by oxidative addition of HSnPh_3 and formation of Pd^{IV} intermediates **7** and **9** or by formation of transient species **10** and **11** if the catalysis proceeds *via* a concerted σ -bond metathesis mechanism (Scheme 2). The former mechanism is supported by the fact that formation, *via* oxidative additions at a Pd(II) centers, of organopalladium(IV) intermediates including hydrido complexes is now well-established.²⁵ On the other hand, a σ -bond metathesis mechanism has recently been invoked for the dehydropolymerization of secondary stannanes catalyzed by zirconocene and hafnocene derivatives^{18b} and described for hydrosilane polymerizations catalyzed by the same complexes.²⁶ Although this mechanism has generally been applied to early transition metals, lanthanides, and actinides,²⁷ recent studies indicate its possible extension to palladium chemistry.²⁸

The combined observations that complexes **6a** and **6b** exhibit the same catalytic activity as the corresponding allyl derivatives **1a** and **1b** and that the trinuclear complex **2a** could be isolated when the reaction with **6a** was quenched after a few minutes strongly indicate that the reactions follow the same pathway for all complexes. The formation of **2a** could either result from HCl elimination (route a, Scheme 3) or from the reaction of the Pd–Cl bond with the tin hydride to afford the transient species **8a**, which would then rapidly react with a second equivalent of HSnPh_3 to yield **2** and H_2 (route b, Scheme 3). Although the former cannot be ruled out, we favor the latter, which also corresponds to part of the proposed catalytic cycle, on the basis of the following observations: (i) the pH of the reaction mixture and that of the gas evolving were not acidic, even when the reactions were carried out on a large scale (> 100 mg of catalyst); (ii) tin hydrides, which are known to reduce organic halides, have already been used to prepare metal hydrides from M–Cl complexes, this reaction being accompanied by elimination of $\text{R}_3\text{-SnCl}$.^{15b,29} Since we did not observe any reactivity of the Si–H bond of the siloxy ligand in **1d** nor any Si–H–Pd interaction, we assume that the above discussion can also be applied in this case.³⁰

Isolation of **2a**, even in the presence of a large excess of HSnPh_3 , suggests that its subsequent reaction represents the rate-determining step in the catalytic cycle. Identification, after completion of the catalysis, of

(31) Devylder, N.; Hill, M.; Molloy, K. C.; Price, G. J. *J. Chem. Soc., Chem. Commun.* **1996**, 711.



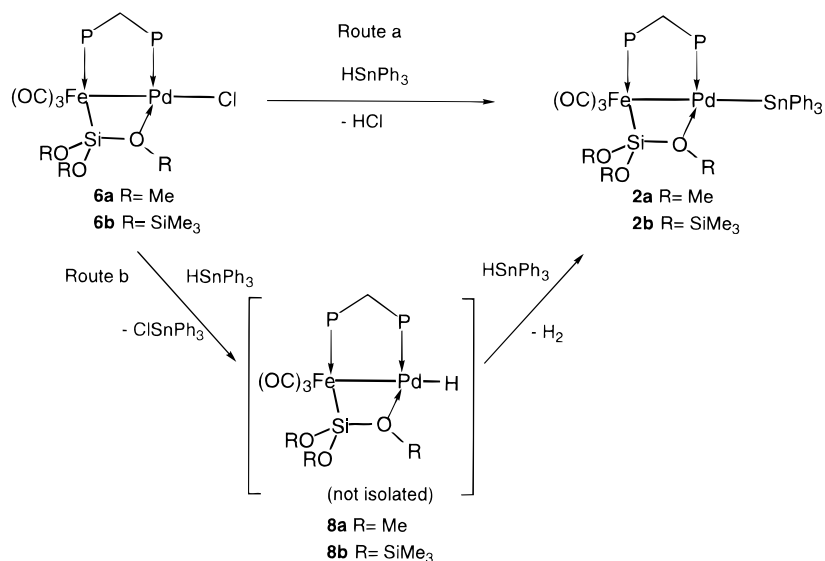
complexes **5**, which are inactive, suggests that one of the factors responsible for the loss of catalytic activity of the bimetallic complexes is the occurrence of Fe–Pd bond cleavage. We could not evidence the fate of the palladium center, which might display residual catalytic activity (see below), and found no indication for the formation of colloidal or metallic Pd.

Effect of the Silyl Ligand in the Catalytic Activity of Complexes 1. The most striking feature of the dehydrogenative coupling of H_2SnPh_3 catalyzed by complexes **1** is the considerable difference of reactivity between the alkoxysilyl complex **1a** and the siloxy complexes **1b–d**, as shown in Figure 3. The latter exhibit a catalytic activity that is about twice that of the former, whereas the duration of the reaction does not exceed 1 h, vs more than 48 h for **1a**. As reported above, the proposed mechanism involves the formation of transient Fe–Pd species stabilized by $\mu_2-\eta^2$ -SiO bridges. Due to the reduced O-donor capacity of the siloxy ligand compared to that of an alkoxysilyl ligand, owing to the more electropositive character of the Si atom in the former, the O \rightarrow Pd interaction should be less stabilizing in **2b–d** than in **2a**. This may explain

the lower reactivity of the latter since the coordination site on the palladium, which is required for the catalysis to proceed, is more efficiently masked in **2a** than in the case of the siloxy complexes. This higher degree of stabilization would also account for the enhancement of the lifetime of the alkoxysilyl catalysts and for the possible isolation of **2a** in contrast to its siloxy analogs **2b–d**.

Differences in reactivity are also observed between the siloxy complexes **1b–d**, as shown in Table 1 and Figure 2. The trend is that the reactivity of a complex, expressed by the TON and TOF values, is enhanced when the number of OSiMe₃ groups decreases. The duration of the reaction, which can be related to the lifetime of the catalyst, follows an opposite trend. As an example, the TON and TOF are 30 and ca. 90% higher, respectively, for **1d**, which has only one OSiMe₃ group, than in the case of **1b**, which possesses three OSiMe₃ groups; however, the reaction is over after ca. 0.5 h with the former whereas it lasts over 1 h with the latter. Recent ¹H NMR studies have evidenced a dynamic behavior of the –SiO \rightarrow Pd interactions in related systems resulting in a rapid exchange between

Scheme 3



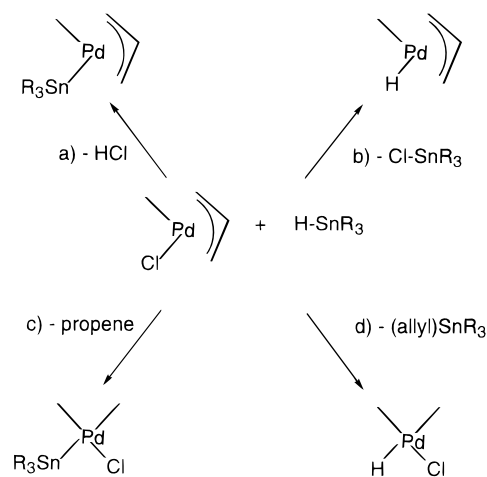
the different OR groups of the silyl ligand which rotates about the Fe–Si bond.^{1a,b} Therefore, from a statistical point of view, intermediates **2** and **9** should be more stabilized by the presence of a tris(siloxy) ligand than by that of mono- or bis(siloxy) one. This difference in stabilization would then account for the observed difference of the reactivity between **1b**, **1c**, and **1d**.

Note that when the Fe–Pt complex [(OC)₃{(Me₃SiO)₃Si}Fe(μ-dppm)Pt(η³-allyl)] (**12**)¹ⁱ was treated with HSnPh₃, no gas evolution nor formation of Sn₂Ph₆ was observed, even after several hours or upon heating (CH₂-Cl₂ reflux). However, this reaction yielded the hydrido complex [HFe{Si(OSiMe₃)₃}(CO)₃(dppm-P)], which has been characterized by ³¹P and ¹H NMR spectroscopy (presence of a doublet due to the hydride at δ = -9.1 ppm, J_{PH} = 27 Hz),^{1a,c} and presumably Pt–Sn complexes, which were not evidenced.

Comparison between Heterobimetallic and Mononuclear Complexes. Previous work by Beletskaya *et al.*¹⁴ has shown that tin hydrides HSnR₃ were dehydrogenated and converted to the corresponding distannanes Sn₂R₆ in the presence of 1 mol % of mononuclear Pd(II) complexes. Although good conversions (*ca.* 80%) were reported, the catalytic activity appears relatively low (TON < 45) in comparison with those observed in the case of the heterobimetallic complexes **1**. However, the authors did not attempt to optimize these reactions, and the experimental conditions are somewhat different from those we have used in the present study. We were, therefore, interested in determining the catalytic activity of a series of mononuclear Pd(II) complexes toward the dehydrogenative coupling of HSnPh₃ in the reaction conditions reported above for complexes **1**. The TONs obtained are given in Table 2. In general, mononuclear Pd(II) complexes appear to be less efficient catalysts than their heterobimetallic counterparts. This observation emphasizes the role of the heterobimetallic structure and more precisely that of the iron fragment, which seems to provide an appropriate environment for the Pd center through metal–metal bonding and the bridging ligands.

Note, however, that the most active mononuclear

Scheme 4



catalysts [Pd(π-allyl)(μ-Cl)]₂ (**13**) and [Pd(π-allyl)Cl-(PPh₃)] (**14**) are slightly more active than the alkoxy-silyl heterobimetallic derivatives **1a**, **2a**, and **6a**. The initial step of the reaction between tin hydrides and complexes **13** and **14** should follow either of the four pathways presented in Scheme 4. Elimination of HCl (pathway a) does not appear likely, since the pH of the reaction mixture was not acidic. From the remaining pathways, we favor b, which involves formation of a stable Sn–Cl bond and maintains the allyl ligand in the coordination sphere of the palladium center. Propene elimination in the cases of complexes **1** resulted from both the allyl ligand being present and the stability of the trinuclear products. One can speculate that the allyl ligand, through an η¹ ⇌ η³ equilibrium, may generate a vacant site on the palladium and thus play a role similar to that of the silyl ligand in **1**. The environment of the palladium(II) center would, therefore, mimic that of the Fe–Pd heterobimetallic complexes, a feature that may account for the higher reactivity of **13** and **14** than the other mononuclear species. The lower TONs for complexes **1a**, **2a**, and **6a** can be attributed to the fact that the Si(OMe)₃ ligand is more stabilizing than the allyl ligand, which in turn may be responsible for their longer lifetime.

Solvent Effects. The catalytic activity of complexes **1** in the dehydrogenative coupling of HSnPh_3 was comparable in Et_2O , toluene, and CH_2Cl_2 . However, in THF, the reaction was less efficient: the TON and the TOF values were 2.5 and 30 times smaller, respectively, than in other solvents, whereas the reaction was already over after 0.5 h (Table 3). It appears reasonable to associate this reduction of catalytic activity with the coordinating properties of THF, which may either coordinate at the palladium center and/or form adducts with the tin hydride, thus rendering the activation of the Sn–H bond less efficient. Surprisingly high TONs were obtained in acetone and were associated with a significant increase of the catalyst lifetime (Table 3). Although the TOF was smaller in acetone than in CH_2Cl_2 or related solvents, the reaction proceeded at a maximum rate for more than 40 min, in contrast in the other cases where it was only maintained for a few seconds. Although we have observed that a small fraction of acetone was reduced by HSnPh_3 with formation of Sn_2Ph_6 and isopropyl alcohol, this side reaction remains a minor process that does not release H_2 and thus did not affect our measurements. Furthermore, we have studied the behavior and stability of **1** and **2a** in acetone and did not find any significant interactions between these complexes and the solvent.

Dehydrogenative Coupling of Other Tin Hydrides. The efficiency of catalysts **1a,b** toward the dehydrogenative coupling of HSnBu_3 was largely enhanced compared to that observed in the case of HSnPh_3 . TON and TOF values were more than 100 times those obtained in the latter case. The difference of reactivity between the alkoxy silyl derivative **1a** and its siloxy analog **1b**, already observed in the presence of HSnPh_3 , still occurred with HSnBu_3 , which indicates the involvement of the silyl unit in the catalytic process as discussed above. The very high reaction rate and the fact that tributyltin units are often involved in radical-mediated reactions may suggest that the catalysis proceeds *via* a radical chain mechanism. However, no modification of the catalytic activity of **1a,b** was noticed when carrying out the experiments in the dark and in the presence of a radical scavenger. Furthermore, we have been able to detect by $^{31}\text{P}\{^1\text{H}\}$ NMR the formation of transient Fe–Pd–Sn trimetallic complex $[(\text{CO})_3\text{Fe}\{\text{Si}(\text{OMe})_2(\text{OMe})\}(\mu\text{-dppm})\text{Pd}(\text{SnBu}_3)]$ (**15**) upon treatment of **1a** with excess HSnBu_3 .^{1b} We assume, therefore, that the reaction proceeds according to a similar catalytic cycle as that presented above for HSnPh_3 and that the enhancement of the TON and TOF values associated with shorter reaction times, compared to experiments carried out with HSnPh_3 , are related to the higher reactivity of intermediates **15** than **2** toward the tin hydride substrate present. The high efficiency of catalysts **1** in the dehydrogenative coupling of HSnBu_3 renders this reaction a competitive approach toward the synthesis of hexa-*n*-butylditin compared to other procedures that usually require harsher conditions or long reaction times or are expensive.

New advances in the synthesis of high molecular polystannanes by either Wurtz coupling³¹ or dehydropolymerization of secondary stannanes¹⁸ have been recently reported. We found, therefore, it of interest to test complex **1b** toward the dehydropolymerization of

H_2SnR_2 (R = Bu, Ph). Surprisingly, in these cases the catalytic activity of **1b** was less than that observed in the presence of the corresponding HSnR_3 . When R = Ph, cyclic oligomers $[\text{SnPh}_2]_n$ ($n = 5$ and 6) were formed, whereas higher molecular weight polystannanes have not been detected. However when R = Bu, both cyclic and linear chains polystannanes were obtained. A relationship between λ_{max} and chain length for $(\text{R}_2\text{Sn})_n$ polymers has recently been presented.³¹ Accordingly, the λ_{max} value we observed at 380 nm is consistent with an unspecified degree of polymerization of greater than 80 Sn atoms. The presence of linear polystannanes is also confirmed by the ^{119}Sn NMR resonance (C_6D_6) at -190 ppm. The other observed λ_{max} values of 350 and 314 nm should correspond to cyclic or linear polystannanes with degrees of oligomerization lower than 15.

Concluding Remarks

In studying the dehydrogenative coupling of tin hydrides catalyzed by heterobimetallic Fe–Pd silyl complexes, we have witnessed that the silyl group played a major role in the catalytic process and that substituent modifications resulted in important variations of catalytic activity and reaction kinetics. The influence of the metal–metal bonding has been evidenced by comparison of the catalytic activity of mononuclear Pd species with that of the title complexes. Owing to different observations made throughout this study, we propose a reaction mechanism in which the bimetallic structure of the catalyst is retained. This work provides an insight into homogenous bimetallic catalysis¹⁹ and illustrates the “ligand effect” that a metal center (*i.e.*, Fe) may have on the adjacent metal (*i.e.*, Pd).

Experimental Section

All of the reactions and manipulations were carried out under an inert atmosphere of purified nitrogen using standard Schlenk-tube techniques. Solvents were dried and distilled under nitrogen before use: hexane and toluene over sodium, tetrahydrofuran and diethyl ether over sodium benzophenone, acetone over calcium chloride, dichloromethane over calcium hydride or phosphorus pentoxide. Nitrogen (Air liquide, R-grade) was passed through BASF R3-11 catalyst and molecular sieves columns to remove residual oxygen and water. Elemental C, H, and N analyses were performed by the Service de microanalyses (Université Louis Pasteur, Strasbourg). Infrared spectra were recorded on a IFS 66 Bruker FT-IR spectrometer. UV–vis spectra were recorded on a Kontron Uvikon 860 spectrometer. The ^1H , $^{31}\text{P}\{^1\text{H}\}$, and $^{13}\text{C}\{^1\text{H}\}$ NMR spectra were recorded at 300.1, 121.5, and 75.5 MHz, respectively, on a Bruker AM300 instrument. Phosphorus chemical shifts were externally referenced to 85% H_3PO_4 in H_2O with downfield chemical shifts reported as positive. Mass spectra were measured on a Fisons ZAB-HF spectrometer (Université Louis Pasteur, R. Hueber). The GPC measurements were recorded on a Chromatograph (vs polystyrene standards) equipped with a refractive index detector and 50, 100, 500, and 10^3 Å PLgel columns in series (tetrahydrofuran solvent). The synthesis of the bimetallic complexes was generally monitored by IR in the $\nu(\text{CO})$ region. $\text{Fe}(\text{CO})_5$ was obtained from Aldrich and used as is. Complexes $[\text{Pd}(\eta^3\text{-allyl})(\mu\text{-Cl})_2]$,^{32a}

(32) (a) Sakakibara, M.; Takahashi, Y.; Sakai, S.; Ishii, Y. *J. Chem. Soc., Chem. Commun.* **1969**, 396. (b) Hartley, F. R. *Organomet. Chem. Rev., Sect. A* **1970**, 6, 119.

$\text{PdCl}_2(\text{PhCN})_2$,^{32b} $[\text{Pd}(\text{mbd})\text{Cl}_2]$,³³ $[\text{PdMeCl}(\text{Ph}_2\text{PCH}_2\text{C}(\text{O})\text{Ph})_2]$,³⁴ **1a**,^{1b} **1b,c**,^{1g} **6a**,^{1a} and **6b**^{1e} were all prepared using published procedures. HSnPh_3 , H_2SnPh_2 , and H_2SnBu_2 were obtained by reduction of the corresponding tin chloride derivatives with LiAlH_4 in diethyl ether.^{18b,37} HSnBu_3 was a commercial sample (Lancaster) and was used as received. The experimental error on the TON and TOF values has been estimated to be 3–4%, values given have been rounded off.

Synthesis of $[(\text{OC})_3\{(\text{Me}_2\text{HSiO})\text{Me}_2\text{Si}\}\text{Fe}(\mu\text{-dppm})\text{Pd}(\eta^3\text{-allyl})]$ (1d**).** A magnetically stirred solution of $[\text{Fe}(\text{CO})_5]$ (0.4 mL, 3 mmol) and $(\text{Me}_2\text{HSi})_2\text{O}$ (1.5 mL, 8.5 mmol) in hexane (100 mL) was irradiated with isopropyl alcohol cooling at 283 K for ca. 5 h. Irradiation was stopped when the $\nu(\text{CO})$ absorptions of $[\text{Fe}(\text{CO})_5]$ (2001 and 2023 cm^{-1}) had almost completely disappeared. The resulting complex *cis*- $[\text{HFe}\{(\text{SiMe}_2(\text{OSiHMe}_2))(\text{CO})_4\}(\nu(\text{CO}) \text{ (hexane) } 2095 \text{ m, } 2029 \text{ sh, } 2021 \text{ vs, and } 2009 \text{ vs } \text{cm}^{-1})$ was not isolated, and the resulting pale-yellow mixture was added immediately to a toluene solution (50 mL) of dppm (1.05 g, 2.73 mmol) in two portions. After each addition, the CO evolved was removed under reduced pressure for 1 min. The solution was stirred for 30 min at room temperature, and the volatiles were removed under reduced pressure, affording *mer*- $[\text{HFe}(\text{CO})_3\{\text{SiMe}_2(\text{OSiHMe}_2)\}(\text{dppm-}P)]$ (**3d**) as a brown solid, which was contaminated by ca. 20% of $[\text{Fe}(\text{CO})_3(\text{dppm-}P)]$ ($^{31}\text{P}\{^1\text{H}\}$ NMR δ 15 ppm).

The hydrido complex **3d** was dissolved in THF and added to a suspension of KH in excess in THF. An immediate gas evolution was noticed (H_2), whereas the color darkened. The formation of transient $\text{K}[\text{Fe}(\text{CO})_3\{\text{SiMe}_2(\text{OSiHMe}_2)\}(\text{dppm-}P)]$ was monitored by IR spectroscopy in the $\nu(\text{CO})$ region (1928 w, 1845 vs, 1824 vs cm^{-1}). When the reaction was complete (after ca. 30 min), the solution was filtered over a 1 cm Celite pad and slowly added to a THF solution of $[\text{Pd}(\eta^3\text{-allyl})(\mu\text{-Cl})_2]$ (0.5 mol equiv) at 233 K. The reaction mixture was allowed to warm to room temperature and stirred for 30 min before it was filtered. The volatiles were removed under reduced pressure, and the residue was chromatographed on alumina. The front band ($R_f = 0.85$) of yellow color containing **1d** was collected and dried *in vacuo*. Complex **1d** was obtained as a yellow-orange air stable powder (yield = 38%; overall yield = 25% based on dppm). IR (THF) 1948 m, 1880 s, 1861 vs cm^{-1} ; ^1H NMR (C_6D_6 , 298 K) δ 0.22 (d, $^3J(\text{H-H}) = 10$ Hz, 6H, $\text{OSi}(\text{H})\text{Me}_2$), 0.48 (s, 6H, Fe-SiMe_2), 2.61 (d, 2H, $^3J(\text{H-H}) = 8.5$ Hz, allyl), 3.48 (br, 1H, allyl), 3.72 (t, 2H, $^2J(\text{P-H}) = 11.5$ Hz, PCH_2P), 5.16 (br, overlapping signals, 2H, allyl, SiH), 5.36 (t, 1H, $^3J(\text{H-H}) \approx ^3J(\text{P-H}) \approx 7$ Hz, allyl), 6.65–7.72 (m, 20H, aromatics); $^{31}\text{P}\{^1\text{H}\}$ NMR (C_6D_6 , 298 K) 26.4 (d, $^{2+3}J(\text{P-P}) = 109$ Hz, P), 66.1 (d, $^{2+3}J(\text{P-P}) = 109$ Hz, P(Fe)). Anal. Calcd for $\text{C}_{35}\text{H}_{40}\text{FeO}_4\text{P}_2\text{PdSi}_2$: C, 52.22; H, 5.01. Found: C, 52.45; H, 4.70.

Spectroscopic data of **3d**: IR (toluene) (also see text) 2050 w, 1980 s, 1965 vs cm^{-1} ; ^1H NMR (C_6D_6 , 298 K) δ -9.1 (d, $J = 26$ Hz, 1H, Fe-H), 0.21 (d, $J = 12$ Hz, 6H, $\text{OSi}(\text{H})\text{Me}_2$), 0.89 (s, 6H, Fe-SiMe_2), 3.18 (dd, $^2J(\text{P-H}) = 8$ and 1 Hz, 2H, PCH_2P), 5.21 (br, 1H, SiH), 6.7–7.7 (m, 20H, aromatics); $^{31}\text{P}\{^1\text{H}\}$ NMR (C_6D_6 , 298 K) -25.34 (d, $J = 105$ Hz, P), 52.18 (d, $J = 105$ Hz, P(Fe)).

Dehydrogenative Coupling of HSnPh_3 Catalyzed by Silylated Heterobimetallic Fe–Pd Complexes and Mononuclear Pd Complexes. General Procedure. A Schlenk flask equipped with a stirring bar and a serum cap was

charged with 1.4 g of HSnPh_3 (4×10^{-3} mol) in 15 mL of solvent and was placed in a water bath at 293 K. CH_2Cl_2 was used as the solvent, except for in the solvent effect studies.

H_2 Monitoring. When the volume of H_2 released (catalyst **1a–d** and solvent effect studies) was monitored, the procedure was as follows: The Schlenk flask was fitted onto a gas burette, and 1 mL of a 5×10^{-4} M solution of catalyst (5×10^{-7} mol) was rapidly added to the reaction mixture *via* syringe through the serum cap. The volumes of H_2 released were directly read on the graduated burette, and the contents of the syringe was taken into account, therefore $V_{\text{H}_2} = V_{\text{read}} - 1 \text{ cm}^3$. The turnover numbers were calculated by the following equation: $\text{TON} = n\text{H}_2/n\text{cat.}$, with $n\text{H}_2$ being determined by applying the gas equation $PV = nRT$. Each experiment was repeated at least 3 times, and the mean values were used for the different plots. When the reaction was over, the volatiles were removed *in vacuo* and the residue washed with Et_2O , affording Sn_2Ph_6 as a white solid (mp = 225–235 $^\circ\text{C}$,³⁸ the ^1H NMR spectrum only showed signals in the aromatic region). The TON determined from the quantity of Sn_2Ph_6 recovered was in almost all cases in good accordance with that determined from the volumes of H_2 . The ether fraction was dried under reduced pressure. Extraction with pentane or hexane afforded a pale yellow solution. The extracts of different experiments with a same catalyst were combined, and the solvent was removed *in vacuo*. NMR spectroscopic analysis of the residues of the reactions carried out with the heterobimetallic Fe–Pd catalysts **1a–c** showed the presence of complexes **5**. Authentic samples of complexes **5a** and **5c** have been prepared independently by reaction of the anions **4a** and **4c** with ClSnPh_3 .²²

$[\text{Ph}_3\text{SnFe}(\text{CO})_3\{\text{Si}(\text{OMe})_3\}(\text{dppm-}P)]$ (5a**).** ^1H NMR (C_6D_6 , 298 K) δ 3.76 (s, 9H, SiOMe), 4.25 (br, 2H, PCH_2P), 6.5–7.7 (m, 35H, aromatics); $^{31}\text{P}\{^1\text{H}\}$ NMR: see text. Anal. Calcd for $\text{C}_{49}\text{H}_{46}\text{FeO}_6\text{P}_2\text{SiSn}$: C, 59.12; H, 4.66. Found: C, 58.95; H, 4.77.

$[\text{Ph}_3\text{SnFe}(\text{CO})_3\{\text{Si}(\text{OSiMe}_3)_3\}(\text{dppm-}P)]$ (5b**).** ^1H NMR (C_6D_6 , 298 K) δ 0.33 (s, 27H, OSiMe_3), 3.28 (d, 2H, $^2J(\text{P-H}) = 8$ Hz, PCH_2P), 6.7–7.7 (m, 35H, aromatics); ^{31}P NMR δ 44.2 (P(Fe), d with Sn satellites, $^{2+3}J(\text{P-P}) = 52$ Hz, $^2J(\text{P-}^{119}\text{Sn}) = 155$ Hz, $^2J(\text{P-}^{117}\text{Sn}) = 130$ Hz), -23.1 ppm (d, $^{2+3}J(\text{P-P}) = 52$ Hz).

$[\text{Ph}_3\text{SnFe}(\text{CO})_3\{\text{SiMe}(\text{OSiMe}_3)_2\}(\text{dppm-}P)]$ (5c**).** ^1H NMR (C_6D_6 , 298 K) δ 0.22 (s, 3H, SiMe), 0.33 (s, 18H, OSiMe_3), 4.27 (d, 2H, $^2J(\text{P-H}) = 11$ Hz, PCH_2P), 6.5–7.9 (m, 35H, aromatics); ^{31}P NMR see text. Anal. Calcd for $\text{C}_{53}\text{H}_{58}\text{FeO}_5\text{P}_2\text{Si}_3\text{Sn}$: C, 58.09; H, 5.34. Found: C, 58.64; H, 5.52.

Sn_2Ph_6 Monitoring. When the formation of Sn_2Ph_6 was monitored (catalysts **1a**, **2a**, and **6a**), the procedure was as follows: a battery of six Schlenk flasks was prepared as described above, except that they were not connected to gas burettes. The catalyst was then added, and the reaction mixtures were successively quenched at $t = 1, 4.5, 8.5, 25, 48$, and 72 h by addition of water. The volatiles were removed under reduced pressure, and the residue was washed with Et_2O , affording pure Sn_2Ph_6 as a white solid, which was weighed. The turnover numbers were determined by the following equation: $\text{TON} = n\text{Sn}_2\text{Ph}_6/n\text{cat.}$

In the case of mononuclear palladium catalysts **13–18**, a battery of three Schlenk flasks was set up as described above. After addition of the catalyst, the reaction mixtures were stirred until the gas evolution had ceased. Sn_2Ph_6 was separated using the same work up as mentioned above.

Dehydrogenative Coupling of HSnBu_3 . The approximate catalytic activity of **1a,b** was first estimated as follows: 1 mL of a 5×10^{-4} M CH_2Cl_2 solution of **1a,b** was added to a Schlenk flask containing 15 mL of CH_2Cl_2 . The flask was

(33) Drew, D.; Doyle, J. R. *Inorg. Synth.* **1972**, *13*, 52.

(34) This complex was prepared according to the procedure described for $[\text{PdCl}_2(\text{Ph}_2\text{PCH}_2\text{C}(\text{O})\text{Ph})_2]$ ³⁵ from $[\text{PdClMe}(\text{cod})]$ ³⁶ and $\text{Ph}_2\text{PCH}_2\text{C}(\text{O})\text{Ph}$.³⁵

(35) Bouaoud, S. E.; Braunstein, P.; Grandjean, D.; Matt, D.; Nobel, D. *Inorg. Chem.* **1986**, *25*, 3765.

(36) Lapido, F. T.; Anderson, G. K. *Organometallics* **1994**, *13*, 303.

(37) Kuivila, H. G.; Sawyer, A. K.; Armour, A. G. *J. Org. Chem.* **1961**, *26*, 1426.

(38) Literature values: (a) 226–228 $^\circ\text{C}$, Gilman, H.; Rosenberg, S. D. *J. Org. Chem.* **1953**, *18*, 1554. (b) 230–234 $^\circ\text{C}$, Tamborski, C.; Ford, F. E.; Soloski, E. J. *J. Org. Chem.* **1963**, *28*, 237.

placed in a 293 K water bath, and *ca.* 2 mL of pure HSnBu₃ was added. An immediate vigorous gas evolution (H₂) was observed, whereas the color of the solution turned red. After the evolution of H₂ had ceased (*ca.* 1 min), another portion of HSnBu₃ was added. This procedure was repeated until the addition of the tin hydride yielded no more H₂. The volatiles were then removed, and the residue was analyzed by ¹H NMR spectroscopy. The ratio between Sn₂Bu₆ and residual HSnBu₃ was determined by integration of the signals in the CH₃ and CH₂ regions, and it was then used to determine the TON, which was found to be >100 000 for **1a** and >200 000 for **1b**. **Bu₆Sn₂**: ¹H NMR (CDCl₃, 298 K) δ 0.91 (t, CH₃), 0.98 (t, CH_{2α}), 1.33 (sext, CH_{2β}), 1.50 (quint, CH_{2β}).

H₂ Monitoring. The procedure described for the dehydrogenative coupling of HSnPh₃ was used. HSnBu₃ (8 g) was placed in a Schlenk flask with 15 mL of CH₂Cl₂ before 0.25 mL of a 2.03 × 10⁻⁴ M solution of **1a** or 0.2 mL of a 9.3 × 10⁻⁵ M solution of **1b** (CH₂Cl₂) was added. A vigorous H₂ evolution was immediately observed in both cases.

Dehydrogenative Polymerization of H₂SnⁿBu₂. Addition of 1 mL of a 3.36 × 10⁻⁴ M CH₂Cl₂ solution of **1b** to 8 g of H₂SnⁿBu₂ in 30 mL of Et₂O resulted in a vigorous gas evolution (the whole vessel was wrapped in an aluminium foil to protect the mixture from room light). Hydrogen evolution slowed down after *ca.* 1 min but continued over the next 2 h. The volume of H₂ released was 169 mL, which corresponded to a TON of *ca.* 20 000, assuming that 1 mol equiv of H₂ was released per catalytic cycle. The experiment was repeated 3 times with 2.4 g of H₂SnⁿBu₂ in order to avoid the presence of unreacted H₂SnⁿBu₂ and thus facilitate the analysis of the product. The average volume of H₂ was 165 mL, and the average TON *ca.* 20 000. After the volatiles were removed under vacuum, the pale brown waxy residue was analyzed.

¹H NMR (300 MHz, benzene-*d*₆) δ 1.03 (br, CH₃, cyclic), 1.15 (br, CH₃, linear), 1.39–1.56 (m, br, CH₂, cyclic), 1.58–1.66 (m, br, CH₂, linear), 1.74–1.98 (m, br, CH₂, cyclic and linear). Assignment made according to ref 18b. UV-vis and ¹¹⁹Sn-¹H} NMR: see text.

Dehydrogenative Polymerization of H₂SnPh₂. The polymerization of H₂SnPh₂ followed procedures similar to that described above for H₂SnⁿBu₂, except that 1 g of H₂SnPh₂ was used per run. A mild gas evolution was noticed, which ceased after 1 h. A pale yellow precipitate was formed. It was separated and washed with pentane. The average *V*_{H₂} = 9.5 mL, and the average mass of [Ph₂Sn]_{*n*} = 100 mg. Assuming that 1 mol equiv of H₂ was released and that one Sn–Sn bond was formed per catalytic cycle, a TON of *ca.* 1100 was determined. IR (KBR) 3061 m, 3045 m, 1641 m, 1572 m, 1476 m, 1425 s, 725 vs, 693 vs, 442 s; ¹H NMR (300 MHz, CDCl₃) δ 7.1–7.8 (m, aromatics); MS (FAB, positive ions; *m/z*) 1251 (Sn₆Ph₇⁺), 895 (Sn₃Ph₇⁺), 861 (Sn₄Ph₅⁺), 741 (Sn₃Ph₅⁺), 700 (Sn₂Ph₆⁺), 623 (Sn₂Ph₅⁺), 546 (Sn₂Ph₄⁺), 469 (Sn₂Ph₃⁺), 351 (SnPh₃⁺), 197 (SnPh⁺). Anal. Calcd for C₁₂H₁₀Sn: C, 52.8; H, 3.69. Found: C, 52.3; H, 3.55.

Acknowledgment. We are grateful to Dr. E. Franta, Mr. R. Meens, and Mr. A. Rameau (Institut Charles Sadron, Strasbourg) for the GPC analyses and to Rhône-Poulenc Chimie and Wacker-Chemie GmbH for the gifts of chemicals. Financial support from the Centre National de la Recherche Scientifique (Paris) and the Ministère de la Recherche et de la Technologie and the Commission of the European Communities (Contract No. CHRX-CT93-0277) are gratefully acknowledged.

OM970353F